

ANALYSIS AND DESIGN OF A GAUSSIAN BACKSCATTER ANTENNA WITH RING FOCUS FEED

W. Thaiwirot and R. Wongsan

School of Telecommunication Engineering, Institute of Engineering
Suranaree University of Technology
Nakhon Ratchasima 30000, Thailand

M. Krairiksh

Faculty of Engineering
King Mongkut's Institute of Technology Ladkrabang
Bangkok, 10520 Thailand

Abstract—This paper presents analysis and design of a Gaussian backscatter antenna with ring focus feed. The curvature of main reflector is Gaussian, and the subreflector is a portion of an ellipse. The antenna has axial symmetry. A backscattering technique is used with the main reflector to achieve wide beamwidth. The input parameters of the proposed antenna are derived in closed form. Physical theory of diffraction (PTD) is used to analyze the radiation pattern of the proposed antenna and verified with experimental results. The effects of the support structures on the radiation patterns of the proposed antenna have been investigated experimentally. The proposed antenna can produce high gain and wide beamwidth (coverage angle $\theta = \pm 65^\circ$). This antenna can be used for realizing earth coverage beam in LEO satellite or indoor wireless LAN applications.

1. INTRODUCTION

Over the last decade, there has been a growing interest in the development of low earth orbit satellite (LEO Satellite) in providing global communication services. Since satellites in low earth orbit change their positions relative to the ground positions quickly, therefore, time

required for ground station-satellite communications is limited. Hence, wide beam antennas are needed. The highly shaped-beam antenna was first developed to give approximately uniform coverage of the earth from satellite antenna [1]. Recently, the similar requirement but different application, a shaped reflector antenna for wireless LAN operating in the millimeter wave, has attracted considerable attentions [2, 3]. However, shaping the reflector to obtain shaped beam yields a discontinuous surface and more complicated manufacturing process. Thaiwirot et al. [4] presented the synthesis of radiation pattern of variety of the shaped backscatters antenna for wide variety of different coverage area. It was found that, the Gaussian backscatter antenna will provide the appropriate characteristics for realizing earth coverage beam in LEO satellite and Wireless Local Area Network (WLAN) application as shown in Fig. 1(a) and Fig. 1(b), respectively. To improve gain and efficiency of reflector antenna, the classical axially symmetric dual-reflector antennas was discussed [5]. It was found that the axially displaced ellipse (ADE antenna) provides an excellent choice for compact high-gain spacecraft antenna applications [6]. This paper presents the axially displaced ellipse antenna. The proposed antenna is a centrally fed displaced axis Gaussian backscatter antenna with a ring focus feed. A backscattering technique is used with the main reflector to achieve wide beamwidth for earth coverage in LEO satellite. Physical theory of diffraction (PTD) is utilized for analysis and design. The input parameters of the proposed antenna are derived in closed form. Experimental results are also presented to verify wide-beam radiation and are in good agreement with the theoretical ones.

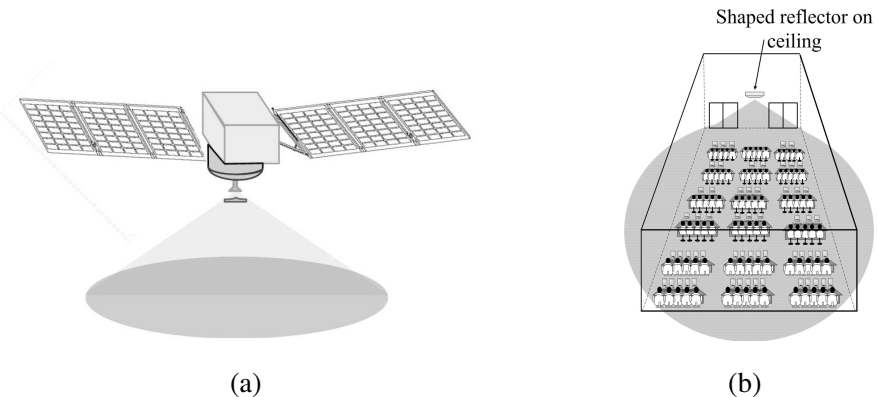


Figure 1. Application of shaped backscatter antenna. (a) Application for LEO satellite. (b) Application for indoor WLAN in the large hall.

2. ANTENNA GEOMETRY AND DESIGN PARAMETER

The cross section of the axially displaced ellipse antenna system is shown in Fig. 2. The antenna has axial symmetry. To understand how this geometry has been derived, we start with the cross section of a Gregorian dual-reflector antenna. The curvature of main reflector is Gaussian, and the subreflector is a portion of an ellipse. The two foci of the ellipse are located at the phase-center of the feed. The three dimensional reflector surface is yielded by spinning the generating curve about the z -axis (symmetry axis). The design procedure in this section is base on [7, 8]. The main reflector and subreflector are defined in their own coordinate system $(O_{MR}, X_{MR}, Y_{MR}, Z_{MR})$ and $(O_{SR}, X_{SR}, Y_{SR}, Z_{SR})$, respectively, and to have a general antenna coordinate system (O, X, Y, Z) in which the main reflector and subreflector are finally expressed. Note that the antenna arrangements we are proposing, $O_{MR} \equiv O_{SR} \equiv O$.

For the classical symmetric Cassegrain or Gregorian reflector antenna, we are dealing with a system of nine parameters defining the overall geometry of the antenna. $D_m, L, A, D_s, \theta_e, L_m, L_s, a$, and f , where (see Figs. 2–4):

D_m : diameter of the main Gaussian backscatter;

L : distance between point and the projection of the bottom-edge of the half-main-reflector onto the axis;

D_s : diameter of the elliptical subreflector;

A : parameter to define the convexity of the main Gaussian backscatter;

θ_e : angle between the Z axis and the ray emanating from the focus, F_0 , of the antenna in the direction of the subreflector edge;

L_m : distance between the focus, F_0 , of the antenna and the projection of the top-edge of the half-main-reflector onto the Z axis;

L_s : distance between the focus, F_0 , of the antenna and the apex of the subreflector;

a and f : parameters defining the geometry of the subreflector.

However, these parameters can not be specified arbitrarily. Therefore, we choose five input parameters, i.e., D_m, A, D_s, L and θ_e to define the antenna, and then calculate from the other design parameters in closed form. These parameters uniquely determine the reflectors and their position in the displaced-axis antenna.

For the definition of the main reflector geometry, we consider only the upper part of the (O_{MR}, X_{MR}, Z_{MR}) plane. The main-reflector

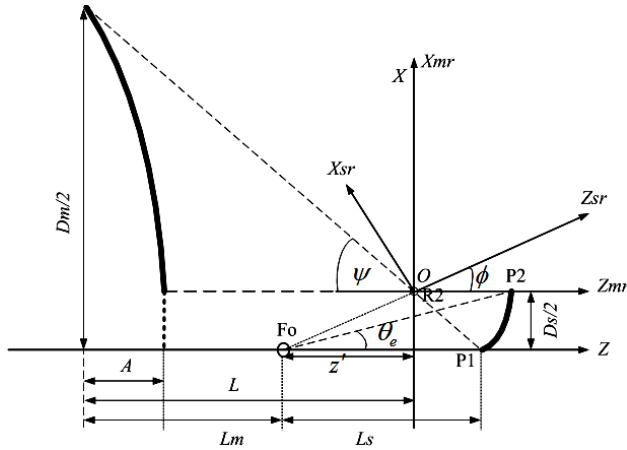


Figure 2. Cross-sectional view of the axially displaced ellipse antenna system.

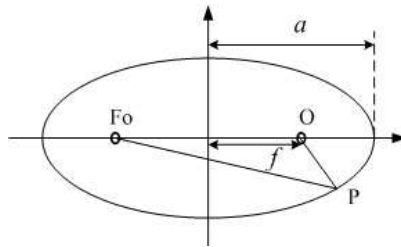


Figure 3. Distance relationship in an ellipse.

profile, $z_{mr}(x_{mr})$, depends on the two real parameters A and L . The equation of a Gaussian backscatter is of the form

$$z_{mr}(x_{mr}) = Ae^{-\left(\frac{2}{D_m}x_{mr}\right)^2} - L, \quad (1)$$

with

$$0 \leq x_{mr} \leq \frac{D_m - D_s}{2}.$$

The elliptical subreflector profile, $z_{sr}(x_{sr})$, is defined in the (O_{SR}, X_{SR}, Z_{SR}) plane, and depends on the two real parameters a and f . It is of the form

$$z_{sr}(x_{sr}) = a\sqrt{1 + \frac{(x_{sr})^2}{f^2 - a^2}} - f. \quad (2)$$

Note: In the case an ellipsoid, $a > f > 0$.

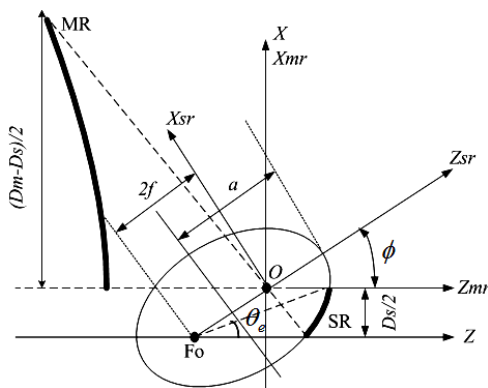


Figure 4. Cross-sectional view of the elliptical-subreflector coordinate system with its parameters.

The points defining the subreflector are such that when x_{sr} is expressed in the main-reflector coordinate system,

$$-\frac{D_s}{2} \leq [x_{sr}]_{\text{Expressed in the MR coordinate system}} \leq 0.$$

To design the antenna, we use the distance relationship in an ellipse [9]. (see Figs. 2–4)

$$\|F_0P\| + \|OP\| = 2a \tag{3}$$

From the five input parameters D_m , A , D_s , L and θ_e , and using the distance relationship in an ellipse in (3), we find that

$$\tan(\psi) = \frac{(D_m - D_s)e}{2(eL - A)}, \tag{4}$$

$$\tan(\phi) = \frac{2}{\left[\frac{\cos(\theta_e)+1}{\sin(\theta_e)} - \frac{\cos(\psi)+1}{\sin(\psi)} \right]}, \tag{5}$$

$$f = \frac{D_s}{4 \sin(\phi)}, \tag{6}$$

$$a = \frac{D_s}{8} \left[\frac{\cos(\theta_e) + 1}{\sin(\theta_e)} + \frac{\cos(\psi) + 1}{\sin(\psi)} \right], \tag{7}$$

$$L_s = 2f \cos(\phi) + \frac{D_s}{2 \tan(\psi)}, \tag{8}$$

$$L_m = L - \frac{D_s}{4} \left[\frac{\cos(\theta_e) + 1}{\sin(\theta_e)} - \frac{\cos(\psi) + 1}{\sin(\psi)} \right] + A. \tag{9}$$

The parameters necessary to represent the axially displaced ellipse reflector antenna system are defined.

3. THEORY

Efficient and accurate high frequency diffraction analysis techniques have been of interest for many years. One of technique that has been widely used in the analytical determination of the radiation patterns of reflector antennas is physical optics (PO). It has the popularity due to its simplicity in the algorithm and regularity of predicted fields. However, physical optics may not be accurate in the prediction of the radiated field in the far-angle regions, the cross-polarized field, or the near-field. Therefore, it may be necessary to use other techniques to accurately compute these quantities. High frequency (HF) diffraction is known as local phenomena, and only part of the scatter contributes to the field such as the edge, corner and specular reflection point etc. Keller's GTD is one of the techniques that can be used to accurately predict the fields in far angle regions [10]. This simple and accurate algorithm has been further enhanced by the development of the Uniform Geometrical Theory of Diffraction (UTD) [11] and the Uniform Asymptotic Theory (UAT) [12]. However, the caustic singularity of GTD, which causes difficulty in the antenna directivity calculation, still exists in the uniform versions. If one uses GTD and PO jointly to overcome this singularity in the reflector analysis, it is usually difficult to determine an observation angle at which a changeover between these two methods should take place. Furthermore, when applied to scatterers with curved surfaces and edges, the computation efficiency of the GTD techniques degrades if the reflection and diffraction points on the scatterers must be determined numerically. Due to these facts, it is desirable to have a diffraction technique by which both of the co-polarized and the cross-polarized fields can be predicted accurately and uniformly over the whole angular range.

Another technique developed at same time as GTD is the Physical Theory of Diffraction (PTD) pioneered by Umfimtsev [13]. Two important modifications to the original PTD have been achieved. The first one is the application of the concept of equivalent edge current (EEC) which eliminates the caustic singularities in the original ray tracing PTD. The second one is an extension for observation angles, which are not on the positions of angle of Keller's cone. Ando's modified PTD is one modification that uses the concept of EEC [14]. A theoretical examination of this method can be found in [15]. Mitzner, on the other hand, did not use EEC explicitly but rather expressed the PTD correction fields in terms of incremental length diffraction coefficients (ILDC) [16]. The third modified PTD that will be studied in this paper is Michaeli's work. He derived the GTD equivalent edge

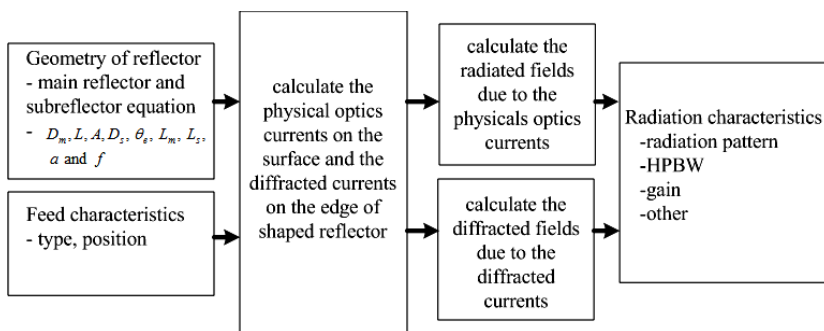


Figure 5. Analytical procedure for physical theory of diffraction.

currents by asymptotically reducing the surface to edge integral [17]. These currents were then written in terms of diffraction coefficients. It has been pointed out in [18] that if the PO components are subtracted from Michaeli’s total scattered field, the fringe fields constructed by Mitzner’s ILDC are recovered. The equivalence of the total scattered field to the sum of the PO and fringe fields has also been observed in the spectral domain [19]. Later, Michaeli evaluated the fringe current radiation integral over the “ray coordinate” instead of over the “normal coordinate”. This improvement using such techniques corrected many of the singularities in Mitzner’s ILDC [20].

The PTD is an integrative technique in which the PO current on a discontinuous perfect conductor surface is refined by the addition of a so-called “nonuniform” component due to the presence of the (edge) discontinuity. The analytical procedure is shown in Fig. 5.

3.1. The Physical Optics (PO) Field

The PO expression for the electric fields radiated from the reflector surface is given by

$$\vec{E}^{PO}(\vec{r}) = -j\omega\mu \frac{e^{-jkr}}{4\pi r} \iint_{\Sigma} \left[\vec{J}^{PO} - \left(\vec{J}^{PO} \cdot \hat{r} \right) \hat{r} \right] e^{jk\hat{r} \cdot \vec{r}'} d\Sigma', \quad (10)$$

or

$$\vec{E}^{PO}(\vec{r}) = -j\omega\mu \frac{e^{-jkr}}{4\pi r} \left(\vec{I} - \hat{r}\hat{r} \right) \cdot \iint_{\Sigma} \left(\vec{J}^{PO} \right) e^{jk\hat{r} \cdot \vec{r}'} d\Sigma', \quad (11)$$

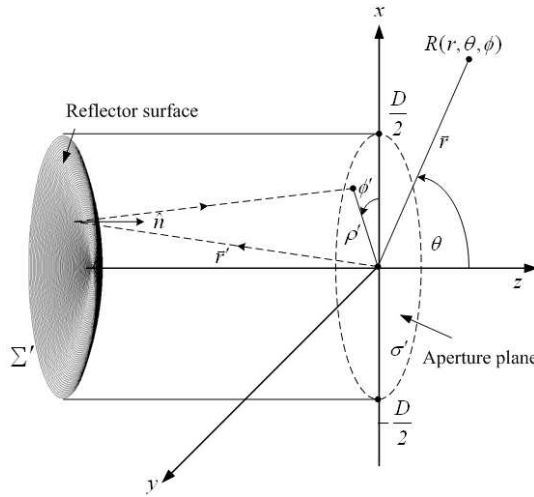


Figure 6. Three-dimensional geometry of a reflector and its parameters.

where $\vec{J}^{PO} = 2\hat{n} \times \vec{H}^i$ is the physical optics currents, \vec{H}^i is incident magnetic fields from feed, \hat{n} is a unit normal to the surface, \vec{I} is the unit dyad, $\vec{r}'_{\Sigma} = x\hat{x} + y\hat{y} + z\hat{z}$ describes the points on reflector surface, \vec{r} describes the observation points, the unit vector \hat{r} represents the corresponding observation direction, as shown in Fig. 6.

3.2. The Fringe Field

As well know, PTD should be included to complement PO solution. In the PTD, the PO field is modified by a fringe field obtained by a one-dimension integration of the equivalent fringe currents along the reflector surface edge. The popular PTD technique is the Michaeli's equivalent edge currents. The fringe fields radiated from the edges of the reflector can be obtained by

$$\vec{E}^f \cong jk \int_C \left[ZI^f(\vec{r}')\hat{s} \times (\hat{s} \times \hat{e}) + M^f(\vec{r}')\hat{s} \times \hat{e} \right] G(\vec{r}', \vec{r}) dl \quad (12)$$

In Michaeli's equivalent edge currents, the final expressions for the electrical equivalent fringe current (I^f) and the magnetic equivalent

fringe current (M^f) [20] as

$$\begin{aligned}
 I^f &= (E_o^i \cdot \hat{e}) \frac{2j}{Zk \sin^2 \beta'} \frac{\sqrt{2} \sin\left(\frac{\phi'}{2}\right)}{\cos \phi' + \mu} \left[\sqrt{1 - \mu} - \sqrt{2} \cos\left(\frac{\phi'}{2}\right) \right] \\
 &+ (H_o^i \cdot \hat{e}) \frac{2j}{k \sin \beta'} \frac{1}{\cos \phi' + \mu} \cdot [\cot \beta' \cos \phi' + \cot \beta \cos \phi \\
 &+ \sqrt{2} \cos\left(\frac{\phi'}{2}\right) (\mu \cot \beta' - \cot \beta \cos \phi) (1 - \mu)^{-\frac{1}{2}}], \quad (13)
 \end{aligned}$$

$$M^f = (H_o^i \cdot \hat{e}) \frac{2jZ \sin \phi}{k \sin \beta \sin \beta'} \frac{1}{\cos \phi' + \mu} \times \left[1 - \sqrt{2} \cos\left(\frac{\phi'}{2}\right) (1 - \mu)^{-\frac{1}{2}} \right], \quad (14)$$

where

$$\begin{aligned}
 G(\vec{r}', \vec{r}) &= \frac{e^{-jks}}{4\pi s}, \quad \mu = \frac{\cos \gamma - \cos^2 \beta'}{\sin^2 \beta'}, \\
 \cos \gamma &= \sin \beta' \sin \beta \cos \phi + \cos \beta' \cos \beta, \\
 \beta &= \pi - \cos^{-1}(\hat{s} \cdot \hat{e}), \quad \beta' = \pi - \cos^{-1}(\hat{s}' \cdot \hat{e}), \\
 \hat{\phi} &= \frac{\hat{s} \times \hat{e}}{\|\hat{s} \times \hat{e}\|}, \quad \hat{\phi}' = \frac{\hat{e} \times \hat{s}'}{\|\hat{e} \times \hat{s}'\|}, \quad \hat{\beta} = \hat{s} \times \hat{\phi}, \quad \hat{\beta}' = \hat{s}' \times \hat{\phi}', \\
 \phi &= \begin{cases} \cos^{-1}(\hat{n} \cdot \hat{\phi}) & \hat{t} \cdot \hat{\phi} \leq 0 \\ 2\pi - \cos^{-1}(\hat{n} \cdot \hat{\phi}) & \hat{t} \cdot \hat{\phi} > 0 \end{cases}, \\
 \phi' &= \begin{cases} \cos^{-1}(\hat{n} \cdot \hat{\phi}') & \hat{t} \cdot \hat{\phi}' \leq 0 \\ 2\pi - \cos^{-1}(\hat{n} \cdot \hat{\phi}') & \hat{t} \cdot \hat{\phi}' > 0 \end{cases}.
 \end{aligned}$$

\hat{s}' is the unit vector from the feed to the edge, \hat{s} is the unit vector from the edge to the observer, k is the wavenumber of the incident wave, Z is the intrinsic impedance of the medium, \vec{r} and \vec{r}' are the position vectors of the observation point and a point on edge C , respectively. Where dl is the increment of arc length l along edge of reflector C , $\hat{e} = -\vec{r}' / \|\vec{r}'\|$ is the unit vector tangent to the edge, \hat{n} is the unit normal vector to the edge, $\hat{t} = \hat{e} \times \hat{n}$ is the unit tangent vector outward from the edge to surface, \vec{E}_o^i and \vec{H}_o^i denote the incident electric and magnetic field vector, respectively, as shown in Fig. 7.

In Mitzner's, Michaeli's and Ando's methods, the total scattered field $\vec{E}^{\rightarrow PTD}$ is constructed by adding a fringe field \vec{E}^f in (12) to the physical optics field $\vec{E}^{\rightarrow PO}$ in (11) [21] as

$$\vec{E}^{\rightarrow PTD} = \vec{E}^{\rightarrow PO} + \vec{E}^f. \quad (15)$$

The radiation fields of the proposed antenna can be obtained by the summation of physical optics fields and fringe field.

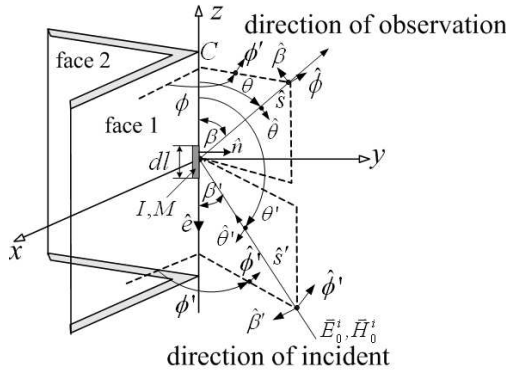


Figure 7. Wedge scattering geometry.

4. NUMERICAL RESULTS

The purpose of the numerical calculation is to illustrate the performance characteristics of the axially displaced ellipse antenna. To illustrate the radiation pattern of proposed antenna, we need to choose five input parameters, i.e., diameter of the main Gaussian backscatter (D_m), diameter of the elliptical subreflector (D_s), parameter to define the convexity of the main Gaussian backscatter (A), parameter to define distance between main reflector and subreflector (L), and the angle θ_e . The design of an antenna has been carried out at 18.75 GHz. The conical horn has been used to feed the antenna. For choosing the input parameter, we start with the design of conical horn antenna that diameter has been accepted at 18.75 GHz (5.04 cm). Later, we choose the subreflector and main reflector diameters, values of the D_s/D_m have to provide the main reflector edge illumination around -15 dB. Then, we define the parameter L and the angle θ_e , to start with L between 20–40 cm and θ_e between 10° – 40° . Finally, we iterate those parameters until the desired patterns are obtained. The antenna was designed using the input parameters, i.e., $D_m = 30$ cm, $D_s = 5.6$ cm, $A = 8.2$ cm, and $L = 30$ cm, $\theta_e = 25^\circ$. For values of the D_s/D_m around 0.19 and $\theta_e = 25^\circ$, the main reflector edge illumination is found to be -15 dB. The designed antenna is presented in Fig. 8. These values present small antenna (compact size) with acceptable dimensions intended to provide wide beamwidth for earth coverage in LEO satellite communication.

The proposed antenna is analyzed by using physical theory of diffraction. The radiation pattern of the antenna, without any studs, is shown in Fig. 9. First of all, one observes that the radiation patterns

are symmetry in both the E -plane and H -plane. The maximum gain of the ADE antenna is 12.98 dBi. The gain at $\theta = \pm 65^\circ$ is 7.5 dBi. There is not severe effect of edge effect. In the case of a single Gaussian backscatter antenna, the maximum gain is 7.5 dBi and gain at $\theta = \pm 65^\circ$ is 3.5 dBi. The main conclusion of this brief analysis is that Gaussian backscatter antenna with ring focus feeding produces higher gain and smaller diffraction effects than a single Gaussian backscatter antenna.

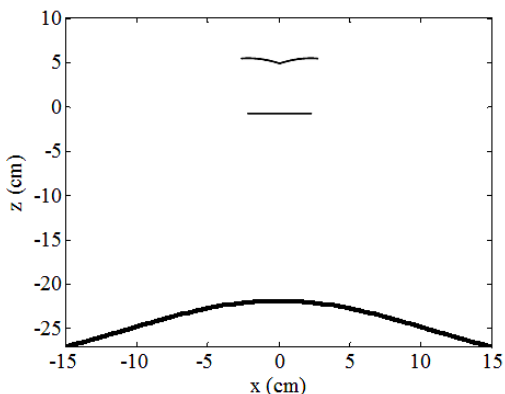


Figure 8. The antenna geometry : $D_m = 30$ cm, $D_s = 5.6$ cm, $A = 8.2$ cm, $L = 30$ cm, $a = 6.4048$ cm, $f = 1.4029$ cm, $L_s = 6.3726$ cm, $L_m = 38.0203$ cm and $\theta_e = 25^\circ$.

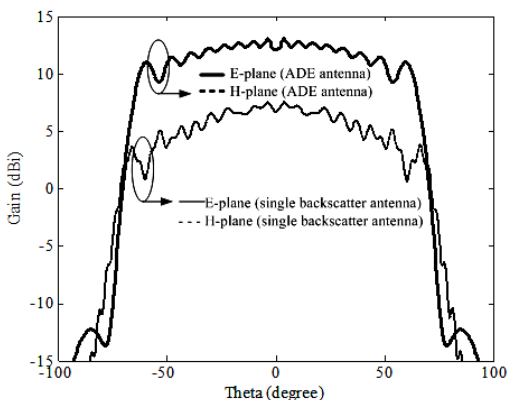


Figure 9. Radiation pattern at 18.75 GHz.

5. MEASURED RESULTS

To verify the performance of the antenna discussed, an antenna prototype has been fabricated on aluminium as shown in Fig. 10. It has an aperture diameter $D_m = 30$ cm, and a subreflector diameter $D_s = 5.6$ cm. In order to compare antenna performance, we consider the two cases of the subreflector support structures. The first case, the subreflector is support from the horn using cylindrical stainless steel studs as shown in Fig. 10(a). The second case, the subreflector is support from the horn using cylindrical superlens cavity with a wall thickness of 0.8 mm as shown in Fig. 10(b). The antenna has been tested in an anechoic chamber.

The measured radiation pattern of the antenna in the first case is plotted together with the simulated pattern as shown in Fig. 11. This plot shows agreement between the measured and simulated both in E -plane and H -plane patterns.

The measured maximum gain in E -plane and H -plane in Fig. 11 are 14.71 dBi and 14.21 dBi, respectively. The gain at $\theta = \pm 65^\circ$ of the measured result is around 4.20 dBi in E -plane and 5.21 dBi in H -plane. It is found that, gain of measured results in E -plane and H -plane are higher than simulated results about 1.73 dBi and 1.23 dBi, respectively. The measured cross-polarization is around 18 dB lower than the co-polarization at $\theta = 0^\circ$. However, the measured radiation patterns show much ripple. This can be explained by reflections occurring between the cylindrical stainless steel studs and the reflector.

An alternative method of supporting the subreflector of ADE antenna is the use of a thin-wall dielectric cylinder (the second case) as shown in Fig. 10(b). The basic problem here is the large variation

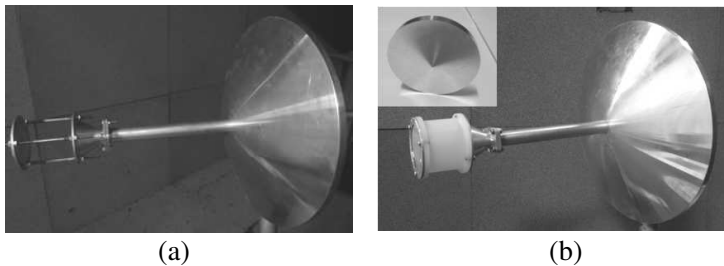


Figure 10. Antenna prototype of the realized 30 cm diameter ADE antenna. Enlarged view of the subreflector is shown inset. (a) Subreflector is supported from the horn using stainless steel studs. (b) Subreflector is supported from the horn using cylindrical superlens cavity.

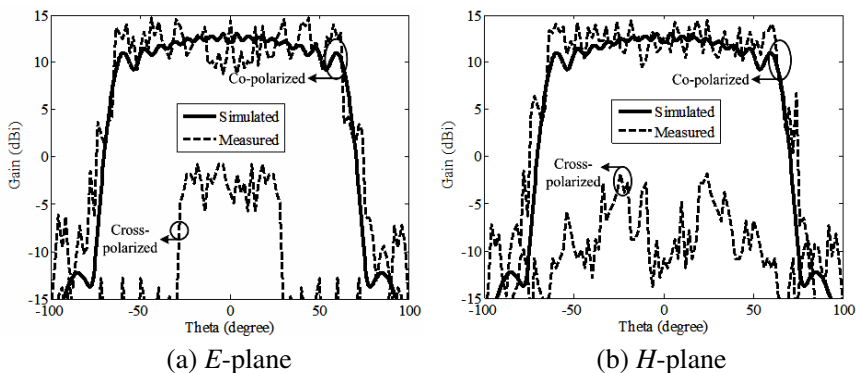


Figure 11. Far field pattern of a Gaussian backscatter antenna with ring focus feed when the subreflector is supported from the horn using stainless steel studs.

in incident angles at the cylinder wall for rays reflected from the subreflector. The effect is minimized by using a material with the smallest possible dielectric constant and thickness. Low loss tangent and high mechanical strength is also desirable. Practical considerations led to the choice of polyamide (nylon-6). This material, popularly called superlene nylon, has a relatively low dielectric constant. The superlene nylon is suitable for this application and can have the small thickness. Fig. 10(b) shows that the subreflector is supported from the horn using cylindrical superlene cavity with a wall thickness of 0.8 mm.

The measured radiation pattern of the antenna in this case is plotted together with the simulated pattern as shown in Fig. 12. This plot shows good agreement between the measured and simulated both in *E*-plane and *H*-plane patterns. The measured maximum gain in *E*-plane and *H*-plane are 14.32 dBi and 14.50 dBi, respectively. The gain at $\theta = \pm 65^\circ$ of the measured result is around 9.21 dBi in *E*-plane and 7.62 dBi in *H*-plane. It is found that, gain of measured results in *E*-plane and *H*-plane are higher than simulated results about 1.34 dBi and 1.52 dBi, respectively. The measured cross-polarization is about 17 dB lower than the co-polarization at $\theta = 0^\circ$. From the radiation patterns in Fig. 11 and Fig. 12, we can observe that subreflector support structures using metallic studs obviously more impact the electrical performance of the antenna than using thin-wall dielectric cylinder. The use of dielectric materials for this support may give better characteristics of the radiation pattern. An additional cause of asymmetry observed in the measured patterns in both cases is (the combination of) the small defocusing and mispointing of the feed, i.e., feed displacements and tilts.

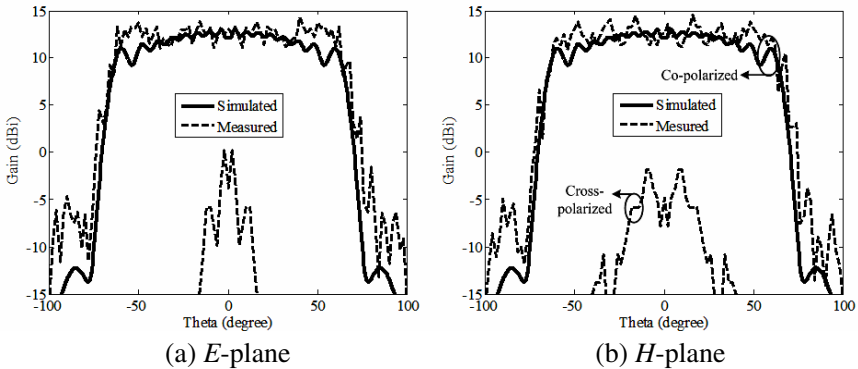


Figure 12. Far field pattern of a Gaussian backscatter antenna with ring focus feed when the subreflector is supported from the horn using using cylindrical superlene nylon cavity.

6. CONCLUSION

The design of quadratic backscatter antenna with ring focus feed (or ADE antenna) was presented. The antenna was analyzed by using the PTD technique. From the simulation results, we can conclude that Gaussian reflector antenna with ring focus feed produces higher gain and smaller diffraction effects than a single Gaussian backscatter antenna. The antenna prototype was fabricated on aluminium by using high-precision CNC machine and measured field patterns in the anechoic chamber. The subreflector support structures by using metallic studs and thin-wall dielectric cylinder have been considered. The measured maximum gain in the case of using metallic tripod support is 14.71 dBi, and the maximum gain at $\theta = \pm 65^\circ$ is around 5.21 dBi. The measured maximum gain in the case of using thin-wall dielectric cylinder support is 14.50 dBi, and the maximum gain at $\theta = \pm 65^\circ$ is around 9.21 dBi. It was found that metallic tripod support obviously impact the electrical performance. The thin-wall dielectric cylinder may give better characteristics of the radiation pattern. Good agreement between simulated and measured results is obtained.

ACKNOWLEDGMENT

I would like to thank the Office of the Higher Education Commission, Thailand for supporting by grant fund under the program Strategic Scholarships for Frontier Research Network for the Joint Ph.D. Program Thai Doctoral degree for this research. Suranaree University of Technology research is also appreciated.

REFERENCES

1. Hay, S. G., D. G. Bateman, T. S. Bird, and F. R. Cooray, "Simple Ka-band earth coverage antennas for LEO satellites," *IEEE Antennas Propag. Soc. Int. Symp.*, Vol. 1, 11–16, 1999.
2. Bird, T. S., J. S. Kot, N. Nikolic, G. L. James, and S. J. Barke, "Millimeter-wave antenna and propagation studies for indoor wireless LANs," *Antennas Propag. Soc. Int. Symp.*, Vol. 1, 336–339, 1994.
3. Smulders, P. F. M., S. Khusial, and M. H. A. J. Herben, "A shaped reflector antenna for 60-GHz indoor wireless LAN access points," *IEEE Trans. on Vehicular Technology*, Vol. 50, 584–591, 2001.
4. Thairvirot, V., P. Krachodnok, and R. Wongsan, "Radiation pattern synthesis from various shaped reflectors base on PO and PTD methods for point-to-multipoint applications," *WSEAS Transactions on Communications*, Vol. 7, 531–540, 2008.
5. Moreira, F. J. S. and A. Prata, Jr., "Generalized classical axially symmetric Dual-reflector antennas," *IEEE Transactions on Antennas and Propagation*, Vol. 49, No. 4, 547–554, 2001.
6. Prata, Jr., A., J. S. Moreira, and L. R. Amaro, "Displace-axis-ellipse reflector antenna for spacecraft communications," *Proceedings SBMO/IEEE MTT-S IMOC 2003*, Vol. 1, 391–395, 2003.
7. Popov, A. P. and T. Milligan, "Amplitude aperture-distribution control in displaced-axis two reflector antenna," *IEEE Antennas and Propag. Magazine*, Vol. 39, No. 6, 58–63, 1997.
8. Granet, C., "A simple procedure for the design of classical displaced-axis dual-reflector antennas using a set of geometric parameters," *IEEE Antennas and Propag. Magazine*, Vol. 41, No. 6, 64–71, 1999.
9. Brown, K. W. and A. Prata, Jr., "A design procedure for classical offset dual-reflector antennas with circular apertures," *IEEE Transactions on Antennas and Propagation*, Vol. 42, No. 8, 1145–1153, 1994.
10. Keller, J. B., "Geometrical theory of diffraction," *J. Opt. Soc. Amer.*, Vol. 52, No. 2, 116–130, 1962.
11. Kouyoumjian, R. G. and P. H. Pathak, "A uniform geometrical theory of diffraction for an edge in a perfectly conducting surface," *IEEE Proc.*, Vol. 63, 1448–1461, 1974.
12. Ahluwalia, D. S., R. M. Lewis, and J. Boersma, "Uniform asymptotic theory of diffraction by a plane screen," *SIAM J. Appl. Math.*, Vol. 16, 783–807, 1968.

13. Ufimtsev, P. Y., "Method of edge waves in the physical theory of diffraction," *Izd-Vo Sovyetskoye Radio*, (Translation prepared by the U.S. Air Force Foreign Technology Division Wright Patterson, AFB, OH, 1971; available from NTIS, Springfield, VA 22161, AD733203), 1–243, 1962.
14. Ando, M., "Radiation pattern analysis of reflector antennas," *Electronics and Communications in Japan*, Part 1, Vol. 68, No. 4, 93–102, 1985.
15. Breinbjerg, O., Y. Rahmat-Samii, and J. A. Appel-Hansen, "Theoretical examination of the physical theory of diffraction and related equivalent currents," Rep. R339, Technical University of Denmark, Lyngby, 1987.
16. Mitzner, K. M. "Incremental length diffraction coefficients," Tech. Rep. AFAI-TR, 73–296, Aircraft Division Northrop Corp., 1974.
17. Michaeli, A., "Elimination of infinities in equivalent edge currents, Part II: Physical optics current components," *IEEE Transactions on Antennas and Propagation*, Vol. 34, No. 8, 1034–1037, 1984.
18. Knott, E. F., "The relationship between Mitzner's ILDC and Michaeli's equivalent currents," *IEEE Transactions on Antennas and Propagation*, Vol. 33, 112–114, 1985.
19. Rahmat-Samii, Y. and R. Mittra, "A spectral domain interpretation of high frequency diffraction phenomena," *IEEE Transactions on Antennas and Propagation*, Vol. 25, 676–687, 1977.
20. Michaeli, A., "Elimination of infinities in equivalent edge currents, Part I: fringe current components," *IEEE Transactions on Antennas and Propagation*, Vol. 34, No.7, 912–918, 1986.
21. Duan, D. W., Y. Rahmat-Samii, and J. P. Mahon, "Scattering from a circular disk: A comparative study of PTD and GTD techniques," *Proceeding of the IEEE*, Vol. 79, No. 10, 1472–1480, 1991.